Optically Induced Degradation Due to Thermally Activated Diffusion in GaN-Based InGaN/GaN MQW Solar Cells

Marco Nicoletto, *Student Member, IEEE*, Alessandro Caria, Carlo De Santi, *Member, IEEE*, Matteo Buffolo, *Associate Member, IEEE*, Xuanqui Huang, Houqiang Fu, *Member, IEEE*, Hong Chen, Yuji Zhao, Gaudenzio Meneghesso, *Fellow, IEEE*, Enrico Zanoni, *Life Fellow, IEEE*, and Matteo Meneghini, *Senior Member, IEEE*

***Abstract*—We extensively investigate the degradation of gallium nitride (GaN)-based high periodicity indium GaN (InGaN)-GaN multiple quantum well (MQW) solar cells submitted to optical stress at high excitation intensity and high temperature. The original results reported in this article indicate the presence of a thermally activated diffusion of impurities from the *p*-side of the devices toward the active region (AR), which favors the increase in the Shockley–Read–Hall (SRH) recombination within the MQWs. Appropriate fitting of the degradation kinetics according to Fick's second law allowed the extrapolation of the diffusion coefficient of the defect involved in the degradation and of the related activation energy. The obtained values suggest that degradation originates from the diffusion of hydrogen. The proposed analytical methodology and the related results provide insight on MQW solar cells degradation and can be used to increase cell performance and reliability in novel applications and harsh environments.**

***Index Terms*—Degradation, diffusion, gallium nitride (GaN), indium gallium nitride (InGaN), multiple-quantum well, solar cells.**

Manuscript received 27 October 2022; revised 10 January 2023; accepted 10 January 2023. Date of publication 20 January 2023; date of current version 24 February 2023. This work was supported in part by the University of Padova through the European Union (Next Generation EU) within the Piano Nazionale di Ripresa e Resilienza (PNRR) Project "Network 4 Energy Sustainable Transition (NEST)"; and in part by the Arizona State University and Rice University through ULTRA, an Energy Frontier Research Center (EFRC) by the U.S. Department of Energy, Office of Science, Basic Energy Sciences under Award DE-SC0021230. The review of this article was arranged by Editor J. D. Phillips. *(Corresponding author: Marco Nicoletto.)*

Marco Nicoletto, Alessandro Caria, Carlo De Santi, Matteo Buffolo, Gaudenzio Meneghesso, and Enrico Zanoni are with the Department of Information Engineering, University of Padova, 35131 Padova, Italy (e-mail: marco.nicoletto.2@studenti.unipd.it).

Xuanqui Huang, Houqiang Fu, and Hong Chen are with the School of Electrical, Computer and Energy Engineering, Arizona State University, Tempe, AZ 85287 USA.

Yuji Zhao is with the School of Electrical, Computer and Energy Engineering, Arizona State University, Tempe, AZ 85287 USA, and also with the Department of Electrical and Computer Engineering, Rice University, Houston, TX 77005 USA.

Matteo Meneghini is with the Department of Information Engineering and the Department of Physics and Astronomy, University of Padova, 35131 Padova, Italy.

Color versions of one or more figures in this article are available at https://doi.org/10.1109/TED.2023.3236915.

Digital Object Identifier 10.1109/TED.2023.3236915

I. Introduction

Understanding the degradation mechanisms of gallium nitride (GaN)-based optoelectronic devices is nowadays of primary importance for the development of reliable LEDs, lasers, photodetectors, and solar cells [1]. Ternary indium GaN (InGaN) alloys have emerged in recent years as promising devices for photovoltaic applications. In particular, InGaN/GaN multiple quantum wells (MQWs) solar cells were proposed as additional components of multijunction (MJ) solar cells, in concentrator solar harvesting systems [2], [3], for wireless power transfer [4] and space applications [5] due to their reliability and efficiency in harsh environments [6]. The suitability of GaN and InGaN for photovoltaic application arises from their unique intrinsic properties, such as a high absorption coefficient, high thermal stability, outstanding radiation resistance, and, in the case of InGaN, a tunable wide bandgap [7], [8].

Until now, the research efforts in developing high-efficiency InGaN solar cells have been mainly focused on improving the material crystal quality, optimizing the structure designs, and controlling the polarization effects [9], [10]. With regard to reliability, a few papers in the literature are focused on the degradation processes induced by high temperatures and by current flow in similar light-emitting GaN-based devices [11], [12]; in contrast, there are no papers that investigate the degradation processes of solar cells or detectors exposed to a continuous high-intensity optical beam, to analyze their behavior in a harsh scenario such as wireless power transfer systems.

The aim of this work is to fill this gap, by investigating the optically induced degradation of GaN-based solar cells with InGaN/GaN MQWs under high-temperature and high-intensity conditions, to evaluate their reliability in the abovementioned applications.

To do so, we performed constant optical power stress tests on GaN-based solar cells with 30 pairs of InGaN/GaN MQWs using a 405-nm laser beam with a constant intensity of 310 W/cm^2 at four different high temperatures, ranging from 135 °C to 205 °C, since the analyzed degradation mode was found to be accelerated by temperature [13]. The main degradation modes exhibited by the devices under investigation (DUTs) are a reduction in short-circuit current (Isc), open-circuit voltage (Voc), external quantum efficiency (EQE), power conversion efficiency (ηOE), and electroluminescence.

Based on the collected experimental evidence, degradation is ascribed to the thermally activated diffusion of impurities

0018-9383 © 2023 IEEE. Personal use is permitted, but republication/redistribution requires IEEE permission.
See https://www.ieee.org/publications/rights/index.html for more information.

Authorized licensed use limited to: Fondren Library Rice University. Downloaded on March 01,2023 at 19:19:03 UTC from IEEE Xplore. Restrictions apply.

Fig. 1. ASU GaN-based solar cell with InGaN-GaN MQWs structure: the thickness and doping of each layer are presented in the figure.

that originate from the p-side of the device and diffuse through the active region (AR) of the solar cell. This process results in an increase in defect density, favoring trap-assisted tunneling mechanisms and nonradiative recombination process.

In addition, we adopted the method proposed van Opdorp and 't Hooft [14], to analyze the time evolution of $1/\tau_{nr}$, thus extracting the diffusion coefficient and the activation energy of these mechanisms. Results support the hypothesis that the diffusion process involves hydrogen ions and help understand for the first time the degradation modes affecting InGaN-based MQWs solar cells submitted to constant optical power stress. Finally, we confirm the critical role of the p-GaN thickness of these devices [15], [16], which depends on the reliability of them in harsh environments.

II. Experimental Details

GaN-based solar cell, with InGaN multiquantum wells, was grown on c-plane (0001) sapphire by conventional metal-organic chemical vapor deposition (MOCVD) (details can be found in [17]). The devices under test (Fig. 1) consist of 2-μm n-GaN (Si doped, 3×10^{18}cm^{-3}) layer over the sapphire substrate and a 125-nm n$^+$-GaN (Si doped, 2×10^{19}cm^{-3}) layer. Above the n$^+$-GaN, the AR was grown, composed by a periodic structure of 30 pairs of undoped $In_{0.15}Ga_{0.85}N$ quantum wells (3 nm) and GaN barriers (7 nm). Above the AR, a 5-nm p-$Al_{0.15}Ga_{0.85}N$ electron blocking layer (EBL) (Mg doped, 2×10^{19} cm^{-3}) is inserted, to enhance carrier collection at the p-side of the devices by reducing the recombination dynamics and increasing the carrier lifetime [17]. Then, a 50-nm p-GaN layer (Mg doped, 2×10^{19} cm^{-3}) and a 10-nm p$^+$-GaN contact layer (Mg doped, $> 2 \times 10^{19}$ cm^{-3}) are formed. A semitransparent 130-nm indium–tin oxide (ITO) layer is deposited by dc sputtering on top of the mesa as a current spreading layer [17] with postannealing in N_2/O_2 at 500 °C. Devices were then processed by standard lithography into 1×1 mm solar cells, and finally, Ti/Al/Ni/Au ring contacts and Ti/Pt/Au grid contacts were deposited via electron beam evaporation around the perimeter and on the top of the mesa, respectively, to form cathode and anode contacts.

Stress and characterization have both been performed on-wafer on a thermally controlled baseplate, heated by a ceramic heater, that allows to regulate the temperature up to 205 °C. Optical excitation was provided by a high-power 405-nm laser diode (nominal output power > 2 W). Details about the setup can be found elsewhere [18]. A portion of the laser beam is redirected to a photodiode to ensure the power stability of the beam over stress time. The stress is performed on four nominally identical samples, under short-circuit conditions, with an optical stress intensity equal to 310 W/cm^2, at four different temperatures: 1) 135 °C; 2) 155 °C; 3) 175 °C; and 4) 205 °C. The stress procedure, which is 100 h long, was divided according to the steps presented in Table I and Fig. 1.

TABLE I
Time Step of the Stress and Total Stress Time at the End of Each Step

Step number	Time step duration [minutes]	Total time stress duration [minutes]
1	30	30
2	30	60
3	60	120
4	180	300
5	300	600
6	600	1200
7	1800	3000
8	3000	6000

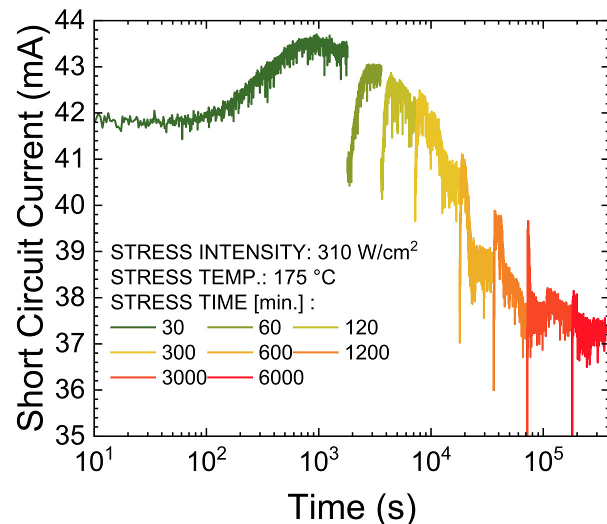

Fig. 2. Short-circuit current measured during the constant power optical stress.

After each step, devices are characterized at 35 °C by means of dark and illuminated current–voltage (I–V) measurements (by using the same laser diode employed during stress for the illuminated I–V), electroluminescence–current (L–I) measurements, and photocurrent measurements. An HP 4145B semiconductor parameter analyzer is used to provide bias to the device and to obtain high-accuracy electrical measurements. Finally, an S130VC photodiode is used for L–I measurements and monochromatic light for photocurrent characterization is generated by a 300-W Xenon arc-lamp whose output is delivered to the sample through a fiber and a proper focusing system.

III. Constant Optical Power Stress

For the sake of brevity, in the following, we will present the in-depth discussion on the data related to the stress at the temperature of 175 °C only, which can be considered to be

Authorized licensed use limited to: Fondren Library Rice University. Downloaded on March 01,2023 at 19:19:03 UTC from IEEE Xplore. Restrictions apply.

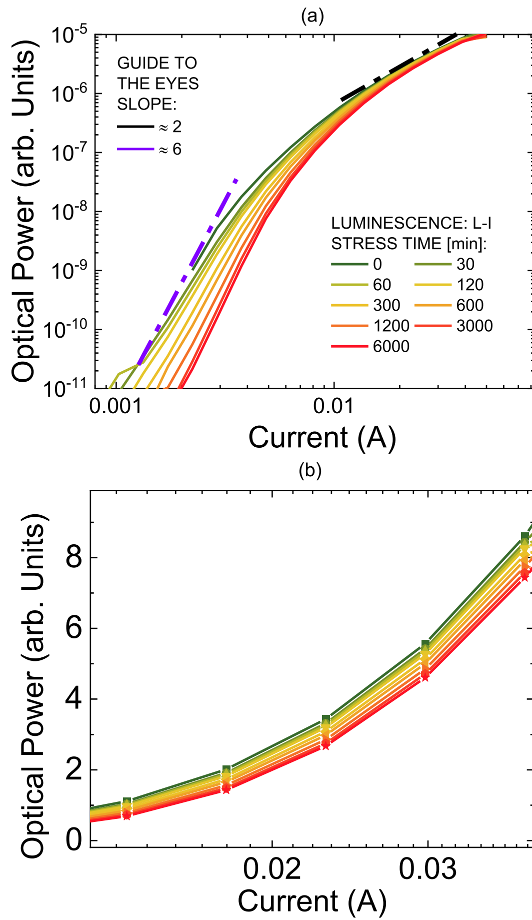

Fig. 3. (a) Optical power measured after each step of the stress (log-to-log scale). Black and purple lines are guide to the eyes. The abnormal slope of the IV curve at low currents is due to asymmetric carriers' injection in the AR. (b) Enlargement of the characteristic for higher currents (linear-to-linear scale).

representative in terms of degradation modes. Fig. 2 shows the trend of the Isc during 100 h of constant optical power stress at a baseplate temperature of 175 °C. After the first 30-min step, the short-circuit current exhibits a slight relative increase of 4%. The initial increase visible at each step of the stress is related to the increased thermionic emission of the carriers photogenerated inside the quantum wells due to device self-heating [18]. However, by observing the steady-state value of Isc during each step, the main outcome of the stress is a decrease in the short-circuit current by 11% with respect to the initial current, which is not recovered at the end of a poststress rest period of 100 h, as is the case for all other degraded cell performances discussed later.

Another significant result of the stress is presented in Fig. 3(a) and (b), where the electroluminescence versus current, measured at 35 °C at the end of each step stress, is shown. The EL signal is analyzed to achieve information on the carrier recombination dynamics, which may impact the overall cell efficiency. A strong decrease in the luminescence was observed during the stress; at the measuring current of 0.01 A, the luminescence signal decreases by 50%, compared to the unstressed sample.

The decrease in the electroluminescence is visible over the entire measured bias range, but is more evident at low measuring current levels, where the luminescence from the cell is more affected by nonradiative recombination processes

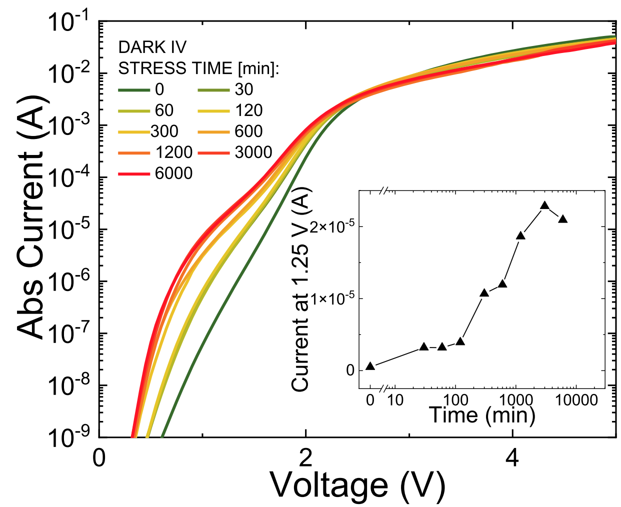

Fig. 4. Dark I–V characteristics at 35 °C after each step of the stress. Inset: current at 1.25 V to better appreciate the current behavior.

due to the impurities present in the AR and by asymmetric injection of carriers occurring within the AR (more on that in Section IV).

The analysis of the dark I–V characteristics reported in Fig. 4 highlights a strong increase in the forward current at low bias level (V < 2 V), just below the diode turn-on. The current flow in these operating conditions is typically mediated by the presence of traps located in the AR, which favor trap-assisted tunneling phenomena [19], [20], [21] as well as other trap-mediated conduction processes [22]. Thus, the increase in the current at the low bias level indicates an increase in the amount of impurities in the AR and, also, the trend of the open-circuit voltage supports these phenomena.

In fact, in a first-order model, the Voc of a solar cell depends on carrier concentration [23], according to

$$V_{\mathrm{OC}} = \frac{kT}{q}\ln\left[\frac{(N_A + \Delta n)\Delta n}{n_i^2}\right] \quad (1)$$

where kT/q is the thermal voltage, N_A is the doping concentration, Δn is the excess carrier concentration, and n_i is the intrinsic carrier concentration.

The Voc of the solar cell, which is presented in Fig. 5, is measured with an excitation intensity of 1 W/cm^2 and shows a decrease from 1.85 V, for the unstressed device to 1.5 V, measured after the last step of the stress decrease. Considering that no variation in the shunt or series resistance is observed, we hypothesized that the decrease in the open-circuit voltage is due to an increase in the amount of nonradiative defects in the AR. This leads to a reduction in the excess carrier concentration [24] and to a consequent deterioration of the abovementioned characteristics.

Additional detail was obtained through the analysis of the variation of the leakage current: the inset of Fig. 4 reports the time dependence of the leakage current measured at 1.25 V. During stress, leakage current increased by two orders of magnitude with respect to the unaged sample; the trend could be fit by a power law, with exponent 0.58, which is consistent with a diffusion process. In fact, a 1-D diffusion process would give a square-root dependence on time, which can be described as

$$R(t, x) = R_0 \mathrm{erfc}\left(\frac{x}{2\sqrt{\mathrm{Dt}}}\right) \quad (2)$$

Authorized licensed use limited to: Fondren Library Rice University. Downloaded on March 01,2023 at 19:19:03 UTC from IEEE Xplore. Restrictions apply.

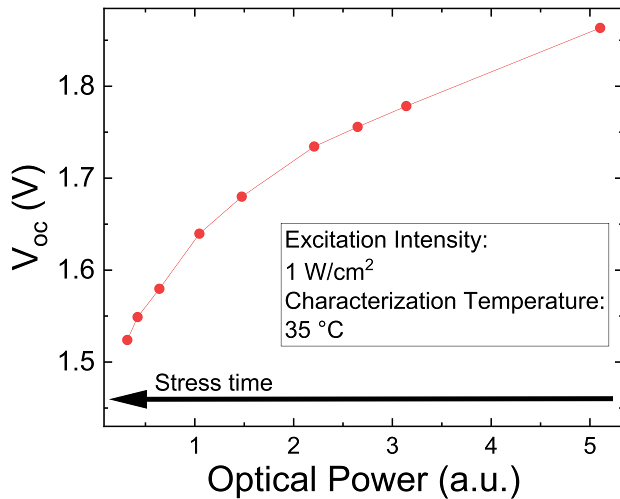

Fig. 5. Voc decrease plotted in a function of the decrease in the optical power.

where $R(t, x)$ is the impurity concentration at time t and position x, $R_0 = R(t = 0)$ is the concentration at source which is considered constant, and D is the diffusion coefficient [25]. Further details on this interpretation are given in the following sections.

IV. Models for Analysis

It has been proposed that the increase in the density of nonradiative recombination centers (NNRCs) is related to the diffusion of impurities toward the AR of the devices [26], [27]. For instance, earlier reports suggested that the diffusion of Mg along dislocations [26], [28] and/or H [25] could cause the gradual degradation of optoelectronic GaN devices. Despite this, an in-depth analysis of diffusion process in GaN-based solar cells was never performed.

Taking into account that hydrogen has been proposed as a candidate diffusant involved in the degradation of InGaN-based devices [24] and many H atoms are incorporated into the p-type layers (doped with a Mg density of 10^{18}–10^{19} cm^{-3}) during MOCVD growth, the hydrogen density remains high even after Mg activation annealing [30], and we supposed that Mg, H, and other impurities such as gallium vacancies (which can originate at the ITO/p+-GaN interface [29]) and also oxygen (which can come from the ITO layer [31]) can easily diffuse in GaN, also through threading dislocations [32], from the final p-GaN layers of the device to the AR, in a thermal-activated diffusion process.

To investigate the impurities involved in the diffusion process, we exploit the model proposed by van Opdorp and 't Hooft [14], which allows to extract the nonradiative recombination lifetime τ_{nr} from the analysis of the subthreshold L–I data. By considering the EQE, η_{ex}, we can obtain the value of τ_{nr} by rewriting

$$\frac{1}{\eta_{ex}} = \frac{(I/q)}{(L/\text{hv})} = \frac{1}{C\eta_i} + \frac{1}{\tau_{nr}\eta_i}\sqrt{\frac{V}{\text{FB}}}\frac{1}{\sqrt{L/\text{hv}}} \quad (3)$$

where q is the elementary electric charge, V is the total volume of the InGaN wells, B is the bimolecular recombination coefficient, hv is the photon energy of emitted light, η_i is the carrier injection efficiency, and F is a parameter, which is proportional to the light extraction efficiency.

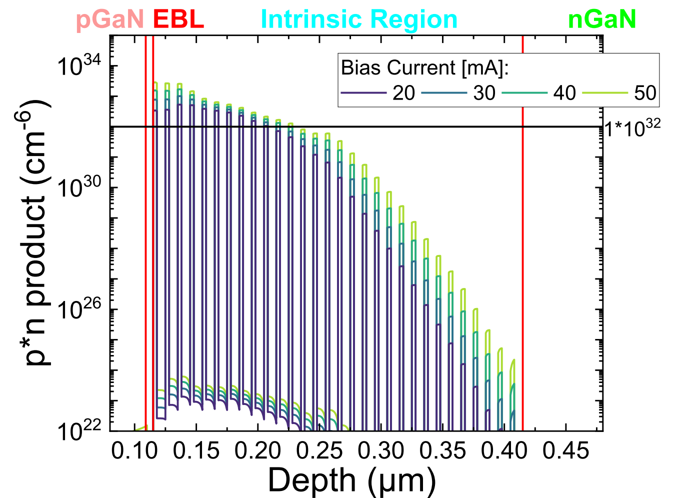

Fig. 6. Simulation of the AR of the device considering hole and electrons product from numerical simulations.

This model has been previously applied to InGaN-based laser diodes: to adapt the model to the InGaN/GaN MQWs solar cells studied in this work, some considerations need to be considered.

A critical parameter for using this method is the active volume V, which is the volume of the region where carriers can radiatively recombine during an L–I measurement. On a system with several quantum wells, the rate of carrier injection can be strongly asymmetric for the various wells and change with increasing injection current. To address this issue, technology computer aided design (TCAD) simulations were carried out, and the electron/hole concentrations in the wells were evaluated. In Fig. 6, the calculated value of the product of electron and hole densities ($n \cdot p$) is reported, at different current regimes (the same current range as in the inset in Fig. 3).

From the simulation results, it is clear that – due to the large number of quantum wells – there is a strongly asymmetric carrier injection. In a first-order approach, we consider the active volume of the devices to be equal to the volume of the quantum wells where $n \cdot p$ is higher than 1% of the peak value. This corresponds to considering that only regions with an $n \cdot p$ product higher than 10^{32} cm^{-6}, corresponding to the first wells near the p-side of the device, effectively contribute to the optical emission from the device. This assumption, based on calculations, is rather realistic and is consistent with the limited injection efficiency of holes in the wells far from the p-side of the device [29], [30].

Considering the continuity equation

$$\frac{J \cdot \eta_{\text{inj}}}{\text{qd}} = \text{An} + \text{Bn}^2 + \text{Cn}^3 \quad (4)$$

where J is the current density, η_{inj} is the injection efficiency, A is the Shockley-Read-Hall (SRH) recombination coefficient (proportional to N_T), B is the bimolecular recombination coefficient, C is the Auger coefficient, and d is the thickness of the AR, and we are interested in evaluating the SRH coefficient. In the current regime where the nonradiative SRH recombination prevails, Bn^2 and Cn^3 can be neglected, and therefore, the carrier density becomes proportional to the injected current; thus, the emitted optical power (Bn^2) is proportional to the square of the injection current: $L \propto I^2$ [31].

Authorized licensed use limited to: Fondren Library Rice University. Downloaded on March 01,2023 at 19:19:03 UTC from IEEE Xplore. Restrictions apply.

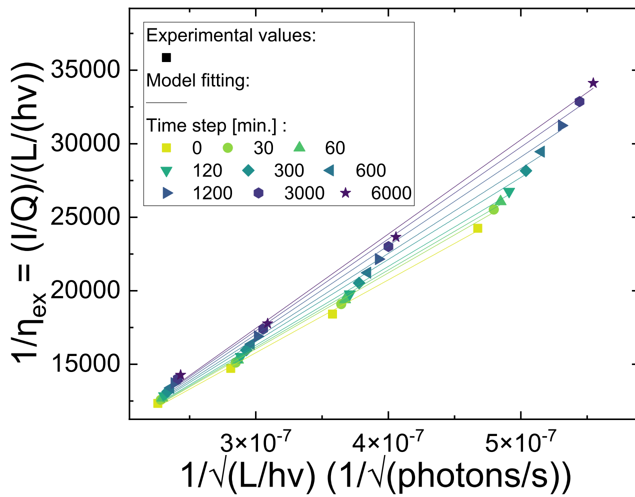

Fig. 7. Replotting of the L–I curves based on the van Opdorp and 't Hooft method.

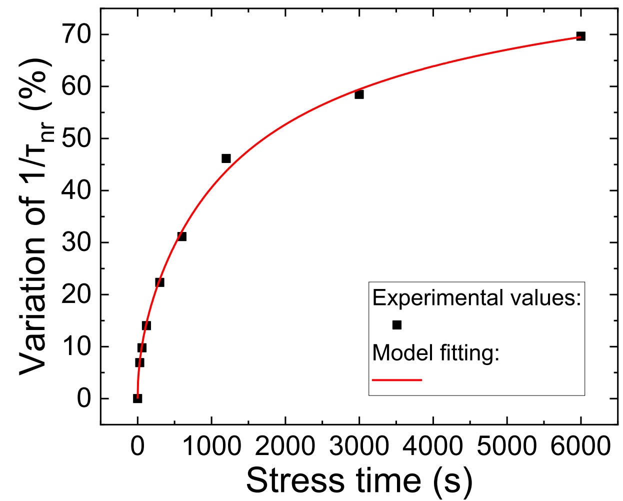

Fig. 8. Trend of the inverse of the nonradiative recombination lifetime estimated after the different steps of the stress.

Considering this, from the L–I slope in Fig. 3(a), SRH recombination dominates only in the current range presented in Fig. 3(b), from 10 to 40 mA, where the slope of L is proportional to the square of the injection current. Thus, we can obtain the value of τ_{nr} related to SRH recombination. By replotting the L–I values in Fig. 3(b) as shown in (3), we obtain that the curve of $1/\eta_{ex}$ versus $(L/\text{hv})^{1/2}$ yields on a straight line (Fig. 7) confirming that the model is suitable in this situation [32], [33].

By fitting the experimental values according to (3), we obtained the SRH recombination losses (i.e., the relative variation of τ_{nr} : $\Delta 1/\tau_{nr}$) during stress time, considering the slope of the fitting lines.

To verify the hypothesis that NRRCs diffusion is involved in the degradation of the device, the time dependence of $1/\tau_{nr}$ is analyzed according to Orita's model [25] assuming that that impurities diffuse from the p-side of the device to the AR. According to (2), considering the concentration of diffusants $N_{\text{diff}}(z)$ and N_0 instead of $R(t, x)$ and R_0, the increase in $1/\tau_{nr}$, at each step of the stress, $\Delta 1/\tau_{nr}$, can be expressed as follows:

$$\Delta 1/\tau_{nr} = \frac{\text{KN}_0}{\text{w}} \int_0^w \text{erfc}\left(\frac{z}{2\sqrt{\text{Dt}}}\right) dz. \tag{5}$$

Here, w is the thickness of the AR, i.e., 300 nm of GaN-InGaN MQWs, and K is a coefficient related to the capture of carriers, which is unknown and thus is considered as a fitting parameter.

To extract the diffusion coefficient, we plot the values of $\Delta 1/\tau_{nr}$, and then, we fit the theoretical values of $\Delta 1/\tau_{nr}$ according to (5) to the experimental results, as shown in Fig. 8. The analysis considers the relative variations of carrier lifetime, rather than the absolute values, with no loss of generality. As can be noticed in Fig. 8, the proposed model can efficiently reproduce the experimental data. For the stress performed at 175 °C, we obtain a value of D that is 1.3×10^{-17} cm^2/s. This value is relatively large for bulk diffusion of impurities in GaN and InGaN at relatively low temperatures: considering the typical values of D for the main impurities in GaN [25], this suggests that hydrogen diffusion is taking place since the high value of estimated D for bulk diffusion cannot be explained if other diffusants are considered. We performed the same experimental investigation and data analysis on three identical samples aged at different temperatures of 135 °C, 155 °C, and 205 °C, to extrapolate the activation energy of the thermally activated diffusion process. Fig. 9 reports the overall results: for a graphical representation, we note here that the values of the diffusion coefficient fall in the light blue region. By decreasing the temperature from 205 °C to 135 °C, we obtain decreasing values of the diffusion coefficients, from 10^{-16} to 10^{-19} cm^2/s. Again, this is consistent with the involvement of H in the diffusion process [25], [34], [35]. The activation energy of the diffusion coefficient that we obtain from this analysis is 1.5 eV.

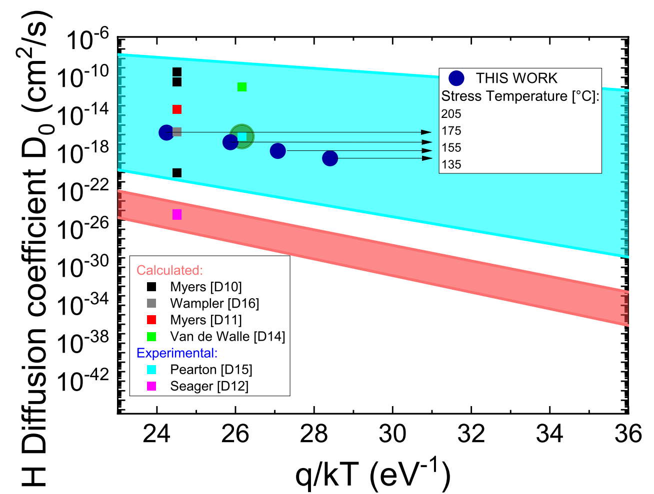

Fig. 9. Experimental (green region) and calculated (red region) diffusion coefficients for hydrogen from literature compared to the data obtained in this work (bigger blue circle). Rearranged from [34].

We note here that the possible trap levels involved in device degradation are likely deep states, rather than shallow levels, since they significantly impact on the SRH recombination coefficient. Such states, which are supposed to be related to hydrogen diffusion, may originate from complexes of gallium vacancies, oxygen and hydrogen, which have been demonstrated to be efficient nonradiative centers in InGaN layers [36].

V. Conclusion

In conclusion, we have investigated the degradation of GaN-based InGaN/GaN MQWs solar cells under constant illumination at different temperatures. The trend of Isc, Voc,

Authorized licensed use limited to: Fondren Library Rice University. Downloaded on March 01,2023 at 19:19:03 UTC from IEEE Xplore. Restrictions apply.

EQE, power conversion efficiency, and electroluminescence of these devices during the stress suggests a thermally activated diffusion process. The time dependence of the extrapolated τ_{nr} is well explained by the proposed model of diffusion-related degradation; by using a simple one-dimensional model, for the first time, we investigated the kinetics of impurity diffusion and extrapolated the related diffusion coefficient, suggesting a role of hydrogen in the degradation process. These results provide insight on the degradation of these devices, which can be useful for lifetime optimization and reliability analysis on InGaN-based devices.

Acknowledgment

The views and opinions expressed are, however, only those of the authors and do not necessarily reflect those of the European Union or the European Commission. Neither the European Union nor the European Commission can be held responsible for them.

References

[1] M. Buffolo et al., "Defects and reliability of GaN-based LEDs: Review and perspectives," *Phys. Status Solidi A*, vol. 219, no. 8, Apr. 2022, Art. no. 2100727, doi: 10.1002/PSSA.202100727.

[2] C. Jiang et al., "Enhanced photocurrent in InGaN/GaN MQWs solar cells by coupling plasmonic with piezo-phototronic effect," *Nano Energy*, vol. 57, pp. 300–306, Dec. 2019, doi: 10.1016/j.nanoen.2018.12.036.

[3] G. Moses, X. Huang, Y. Zhao, M. Auf der Maur, E. A. Katz, and J. M. Gordon, "InGaN/GaN multi-quantum-well solar cells under high solar concentration and elevated temperatures for hybrid solar thermal-photovoltaic power plants," *Prog. Photovolt., Res. Appl.*, vol. 28, no. 11, pp. 1167–1174, Nov. 2020, doi: 10.1002/pip.3326.

[4] C. De Santi et al., "GaN-based laser wireless power transfer system," *Materials*, vol. 11, no. 1, p. 153, Jan. 2018, doi: 10.3390/MA11010153.

[5] Y. Zhao et al., "InGaN-based solar cells for space applications," in *Proc. Midwest Symp. Circuits Syst.*, Sep. 2017, pp. 954–957, doi: 10.1109/MWSCAS.2017.8053083.

[6] D. H. Lien et al., "Harsh photovoltaics using InGaN/GaN multiple quantum well schemes," *Nano Energy*, vol. 11, pp. 104–109, Jan. 2015, doi: 10.1016/J.NANOEN.2014.10.013.

[7] J. Wu et al., "Superior radiation resistance of $In_{1-x}Ga_xN$ alloys: Full-solar-spectrum photovoltaic material system," *J Appl Phys*, vol. 94, no. 10, p. 6477, Oct. 2003, doi: 10.1063/1.1618353.

[8] J. Wu, "When group-III nitrides go infrared: New properties and perspectives," *J. Appl. Phys.*, vol. 106, no. 1, Jul. 2009, Art. no. 011101, doi: 10.1063/1.3155798.

[9] C. J. Neufeld et al., "Effect of doping and polarization on carrier collection in InGaN quantum well solar cells," *Appl Phys Lett*, vol. 98, no. 24, pp. 16–19, 2011, doi: 10.1063/1.3595487.

[10] N. G. Young et al., "High-performance broadband optical coatings on InGaN/GaN solar cells for multijunction device integration," *Appl. Phys. Lett.*, vol. 104, no. 16, Apr. 2014, Art. no. 163902, doi: 10.1063/1.4873117.

[11] M. la Grassa et al., "Ageing of InGaN-based LEDs: Effects on internal quantum efficiency and role of defects," *Microelectron. Rel.*, vol. 55, nos. 9–10, pp. 1775–1778, Aug. 2015, doi: 10.1016/J.MICROREL.2015.06.103.

[12] J. Fu et al., "Degradation and corresponding failure mechanism for GaN-based LEDs," *AIP Adv*, vol. 6, no. 5, May 2016, Art. no. 055219, doi: 10.1063/1.4953056.

[13] A. Caria et al., "GaN-based solar cells degradation kinetics investigated at high temperature under high-intensity 405 nm optical stress," *Proc. SPIE*, vol. 12001, pp. 44–51, Mar. 2022, doi: 10.1117/12.2608680.

[14] C. van Opdorp and G. W.'t Hooft, "Method for determining effective nonradiative lifetime and leakage losses in double-heterostructure lasers," *J. Appl. Phys.*, vol. 52, no. 6, p. 3827, Aug. 1998, doi: 10.1063/1.329845.

[15] A. Caria et al., "Quantum efficiency of InGaN-GaN multi-quantum well solar cells: Experimental characterization and modeling," *J. Appl. Phys.*, vol. 131, no. 22, p. 224501, Jun. 2022, doi: 10.1063/5.0076833.

[16] M. Nicoletto et al., "Characterization and modelling of quantum efficiency InGaN-GaN multi-quantum well (MQW) solar cells," in *Proc. 45th Wocsdice/Exmatec Conf.*, May 2022, pp. 25–26.

[17] X. Huang et al., "Energy band engineering of InGaN/GaN multi-quantum-well solar cells via AlGaN electron- and hole-blocking layers," *Appl. Phys. Lett.*, vol. 113, no. 4, Jul. 2018, Art. no. 043501, doi: 10.1063/1.5028530.

[18] A. Caria et al., "Excitation intensity and temperature-dependent performance of InGaN/GaN multiple quantum wells photodetectors," *Electronics*, vol. 9, no. 11, p. 1840, Nov. 2020, doi: 10.3390/ELECTRONICS9111840.

[19] M. Mandurrino et al., "Physics-based modeling and experimental implications of trap-assisted tunneling in InGaN/GaN light-emitting diodes," *Phys. Status Solidi (A) Appl. Mater. Sci.*, vol. 212, no. 5, pp. 947–953, May 2015, doi: 10.1002/PSSA.201431743.

[20] M. A. der Maur, B. Galler, I. Pietzonka, M. Strassburg, H. Lugauer, and A. Di Carlo, "Trap-assisted tunneling in InGaN/GaN single-quantum-well light-emitting diodes," *Appl. Phys. Lett.*, vol. 105, no. 13, Sep. 2014, Art. no. 133504, doi: 10.1063/1.4896970.

[21] N. Roccato et al., "Modeling the electrical characteristics of InGaN/GaN LED structures based on experimentally-measured defect characteristics," *J. Phys. D, Appl. Phys.*, vol. 54, no. 42, Aug. 2021, Art. no. 425105, doi: 10.1088/1361-6463/AC16FD.

[22] M. Musolino et al., "A physical model for the reverse leakage current in (In,Ga)N/GaN light-emitting diodes based on nanowires," *J. Appl. Phys.*, vol. 119, no. 4, Jan. 2016, Art. no. 044502, doi: 10.1063/1.4940949.

[23] R. A. Sinton and A. Cuevas, "Contactless determination of current-voltage characteristics and minority-carrier lifetimes in semiconductors from quasi-steady-state photoconductance data," *Appl. Phys. Lett.*, vol. 69, no. 17, p. 2510, Aug. 1998, doi: 10.1063/1.117723.

[24] X. Huang et al., "Reliability analysis of InGaN/GaN multi-quantum-well solar cells under thermal stress," *Appl. Phys. Lett.*, vol. 111, no. 23, Dec. 2017, Art. no. 233511, doi: 10.1063/1.5006650.

[25] K. Orita et al., "Analysis of diffusion-related gradual degradation of InGaN-based laser diodes," *IEEE J. Quantum Electron.*, vol. 48, no. 9, pp. 1169–1176, Jun. 2012, doi: 10.1109/JQE.2012.2203795.

[26] O. H. Nam et al., "Characteristics of GaN-based laser diodes for post-DVD applications," *Phys. Status Solidi A*, vol. 201, no. 12, pp. 2717–2720, Sep. 2004, doi: 10.1002/PSSA.200405114.

[27] M. Meneghini et al., "Extensive analysis of the degradation of blu-ray laser diodes," *IEEE Electron Device Lett.*, vol. 29, no. 6, pp. 578–581, Jun. 2008, doi: 10.1109/LED.2008.921098.

[28] S. Tomiya, T. Hino, S. Goto, M. Takeya, and M. Ikeda, "Dislocation related issues in the degradation of GaN-based laser diodes," *IEEE J. Sel. Topics Quantum Electron.*, vol. 10, no. 6, pp. 1277–1286, Nov. 2004, doi: 10.1109/JSTQE.2004.837735.

[29] Y. Kawaguchi et al., "Influence of polarity on carrier transport in semipolar ($202\bar{1}^{-}$) and (202^{-})1) multiple-quantum-well light-emitting diodes," *Appl. Phys. Lett.*, vol. 100, no. 23, Jun. 2012, Art. no. 231110, doi: 10.1063/1.4726106.

[30] D. S. Sizov et al., "Carrier transport in inGaN MQWs of aquamarine- and green-laser diodes," *IEEE J. Sel. Topics Quantum Electron.*, vol. 17, no. 5, pp. 1390–1401, Feb. 2011, doi: 10.1109/JSTQE.2011.2116770.

[31] C. de Santi, A. Caria, F. Piva, G. Meneghesso, E. Zanoni, and M. Meneghini, "Degradation mechanisms of InGaN visible LEDs and AlGaN UV LEDs. LTD," in *Reliability of Semiconductor Lasers and Optoelectronic Devices*. (Woodhead Publishing Series in Electronic and Optical Materials), 1st ed. Padua, Italy: Univ. of Padova, Department of Information Engineering, 2021, pp. 273–312, doi: 10.1016/b978-0-12-819254-2.00001-1.

[32] M. Meneghini et al., "Degradation of InGaN-based laser diodes related to nonradiative recombination," *IEEE Electron Device Lett.*, vol. 30, no. 4, pp. 356–358, Mar. 2009, doi: 10.1109/LED.2009.2014570.

[33] N. Trivellin et al., "Degradation of InGaN-based laser diodes due to increased non-radiative recombination rate," *Phys. Status Solidi A*, vol. 207, no. 1, pp. 41–44, Jan. 2010, doi: 10.1002/PSSA.200982620.

[34] C. De Santi, M. Meneghini, G. Meneghesso, and E. Zanoni, "Degradation of InGaN laser diodes caused by temperature- and current-driven diffusion processes," *Microelectron. Rel.*, vol. 64, pp. 623–626, Sep. 2016, doi: 10.1016/J.MICROREL.2016.07.118.

[35] A. M. Yong, C. B. Soh, X. H. Zhang, S. Y. Chow, and S. J. Chua, "Investigation of V-defects formation in InGaN/GaN multiple quantum well grown on sapphire," *Thin Solid Films*, vol. 515, no. 10, pp. 4496–4500, Mar. 2007, doi: 10.1016/J.TSF.2006.07.181.

[36] C. E. Dreyer, A. Alkauskas, J. L. Lyons, J. S. Speck, and C. G. Van de Walle, "Gallium vacancy complexes as a cause of Shockley-Read-Hall recombination in III-nitride light emitters," *Appl. Phys. Lett.*, vol. 108, no. 14, Apr. 2016, Art. no. 141101, doi: 10.1063/1.4942674.

Authorized licensed use limited to: Fondren Library Rice University. Downloaded on March 01,2023 at 19:19:03 UTC from IEEE Xplore. Restrictions apply.